

# Weakly-supervised Action Localization via Hierarchical Mining

Jia-Chang Feng<sup>1,3</sup>, Fa-Ting Hong<sup>2</sup>, Jia-Run Du<sup>1</sup>, Zhongang Qi<sup>3,4</sup>,  
Ying Shan<sup>3,4</sup>, Xiaohu Qie<sup>4</sup>, Wei-Shi Zheng<sup>1</sup>, Jianping Wu<sup>5</sup>

<sup>1</sup> School of Computer Science and Engineering, Sun Yat-sen University

<sup>2</sup> Department of Computer Science and Engineering, HKUST

<sup>3</sup> ARC Lab, <sup>4</sup> Tencent PCG <sup>5</sup> Tsinghua University

**Abstract.** Weakly-supervised action localization aims to localize and classify action instances in the given videos temporally with only video-level categorical labels. Thus, the crucial issue of existing weakly-supervised action localization methods is the limited supervision from the weak annotations for precise predictions. In this work, we propose a hierarchical mining strategy under video-level and snippet-level manners, *i.e.*, hierarchical supervision and hierarchical consistency mining, to maximize the usage of the given annotations and prediction-wise consistency. To this end, a Hierarchical Mining Network (HiM-Net) is proposed. Concretely, it mines hierarchical supervision for classification in two grains: one is the video-level existence for ground truth categories captured by multiple instance learning; the other is the snippet-level inexistence for each negative-labeled category from the perspective of complementary labels, which is optimized by our proposed *complementary label learning*. As for hierarchical consistency, HiM-Net explores video-level co-action feature similarity and snippet-level foreground-background opposition, for discriminative representation learning and consistent foreground-background separation. Specifically, prediction variance is viewed as uncertainty to select the pairs with high consensus for proposed *foreground-background collaborative learning*. Comprehensive experimental results show that HiM-Net outperforms existing methods on THUMOS14 and ActivityNet1.3 datasets with large margins by hierarchically mining the supervision and consistency. Code will be available on GitHub<sup>1</sup>.

**Keywords:** Weakly-supervised Learning, Action Localization

## 1 Introduction

Action localization is a challenging video understanding problem of detecting and classifying action instances in the given video. To tackle this problem, many methods try to solve it in a fully-supervised manner [42,61,22,20,55], but they rely on massive time-consuming annotations, *i.e.*, start and end timestamps

---

<sup>1</sup> <http://github.com/fjchange/HiM-Net>

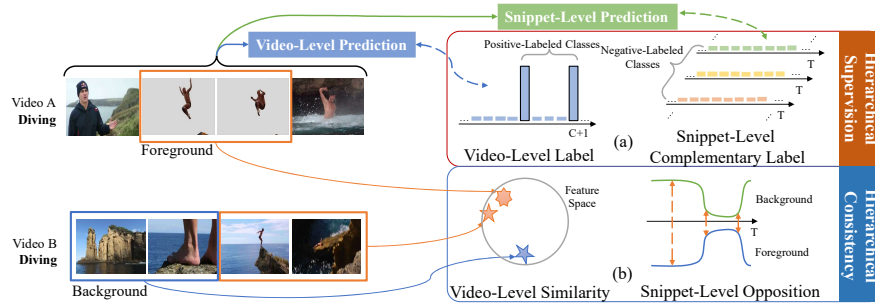


Fig. 1: The motivation of hierarchical mining. (a) **Hierarchical Supervision Mining**: hierarchically leverage the information from the video-level label for positive-labeled classes and snippet-level complementary label for negative-labeled classes. (b) **Hierarchical Consistency Mining**: leverage the consistency in feature similarity between videos with identical category and snippet-level estimation opposition from different branches.

for each action instance. To relieve this issue, researchers pay more attention to weakly-supervised action localization (WSAL) [18,19,8,12,11,25,23,24,29,28,33,34,50,57,56,54,64,14], which explores a more efficient learning strategy with only video-level categorical labels.

As with other weakly-supervised video understanding tasks, *i.e.*, video highlight detection [46,9], video anomaly detection [5,44] and video grounding [60,51], existing WSAL methods [18,19,56,11,34,57] mainly develop their framework based on the multiple instance learning (MIL) paradigm [65]: obtaining a video-level prediction via aggregation and optimization under the video-level supervision. Though MIL-based methods have a large development, they still suffer limited snippet-level optimization signals, leaving highly inferior performance when compared with fully-supervised methods. In consideration of this issue, researchers explore diverse solutions. Some methods [54,11,14] try to erase the most discriminative parts for learning action completeness. Some methods [50,56,36,14] learn with pseudo labels generated by manual thresholds and iterative refinement. Meanwhile, some methods focus on the feature-level manner: feature-level metric learning [12,7,57], uncertainty modeling on feature magnitude [19], and feature re-calibration [8]. Furthermore, external information is used to assist the learning, *e.g.* modality [17], data [58], or annotation [33,29].

However, fine-grained supervision can be obtained from the weak annotations without bells and whistles, but inside the given annotations. Intuitively, it’s expected for the trained prediction reflects the information from annotations in any hierarchy. However, previous works are limited in a video-level manner. As shown in Fig.1(a), the given annotations indicate not only the video-level existence for the positive-labeled categories but also accurate snippet-level inexistence for all negative-labeled categories from the perspective of complementary labels. Concretely, given a video annotated as “Diving”, the annotation can be decomposed into two hierarchies: this video contains “Diving” and “Background” snippets in

a video-level manner as the video-level label, while there is no snippet for the negative-labeled classes like “Long Jump” or “Billiards”, forming snippet-level complementary label. Thus, we decompose the learning process into video-level and snippet-level manners to fully leverage the supervision signals from the weak annotations in both manners. The former leverages MIL [11,18], while for the latter, we propose a *Complementary Label Learning* (CLL) to capture the information in complementary labels to suppress all the unexpected snippet-level activation for better snippet-level classification.

Apart from hierarchical supervision, we aim to mine more optimization signals from the **hierarchical consistency** between two predictions. Recently, some methods explore the cross-modality prediction-wise consistency [56,50,14,8], while some methods explore cross-video co-action feature similarity, which indicates the video-level feature similarity between two videos with the same action category [38,12,7,48,31,8]. Here, we also adopt this video-level co-action similarity learning (VCL) for discriminative representation. Indeed, there remains a snippet-level foreground-background consistency as shown in Fig.1(b), especially for the attention-based method with external background class [18,11,8,14]. In these methods, the attention branch generates foreground estimation while the classification branch generates background one. Intuitively, they should perform oppositely, performing as the pseudo targets of the other. As the label noise is inevitably in two estimations, selecting the reliable pseudo targets is important to leverage this consistency. Instead of aligning them directly or via pseudo labels [56,50], we propose snippet-level foreground-background collaborative learning (SCL) that selects the pseudo targets by treating prediction variance as uncertainty [62,63]. With the help of uncertainty, the collaborative learning process can perform adaptively on terms with high consensus.

In this work, we propose a Hierarchical Mining Network (HiM-Net) to mine the hierarchical supervision and consistency. HiM-Net utilizes the MIL and CLL to mine the supervision hierarchically to fully leverage the given annotations for correct classification of two grains, while SCL and VCL are employed to mine the consistency hierarchically for discriminative representation and consistent foreground-background separation. To validate the effectiveness of our method, we perform experiments on two standard benchmarks, THUMOS14 and ActivityNet1.3. By jointly mining the hierarchical supervision and consistency, our HiM-Net successfully distinguishes action instances and achieves the new state-of-the-art on both benchmarks. Overall, our contributions are three-fold:

- We propose to mine hierarchical supervision and consistency for full use of the weak annotations and prediction-wise consistency.
- We propose two kinds of snippet-level mining strategies: a complementary label learning (CLL) to suppress snippet-level unexpected activation, and an uncertainty-aware snippet-level foreground-background collaborative learning (SCL) for mutual promoting the foreground-background separation.
- Our method not only significantly outperforms state-of-the-art WSAL methods, but also performs comparably with some fully-supervised methods.

## 2 Related Works

- **Fully-supervised Action Localization.** The goal of action localization is to find the temporal intervals of action instances from long untrimmed videos and classify them. To solve this task, many methods require accurate timestamp annotations for each action instance in the given video during training. Several large-scale datasets have been collected for this task, *e.g.* THUMOS14 [15] and ActivityNet [2]. Many methods [42,61,22,6,20,55,47] are based on the paradigm of proposal-then-classification, which generate proposals via bottom-up [61,22,20,55,47,39] or top-down [42,6] manner followed by multi-class classification. Some methods explore a one-stage paradigm, which directly generate class-aware proposals [21,26,49], or group the action and boundary predictions [53].

- **Weakly-supervised Action Localization.** Recently, many researchers attempt to relieve the dependence on temporal annotations by learning with only video-level category labels. Most works focus on utilizing pre-extracted features for both RGB and optical flow modalities and learning with multiple instance learning strategy. Wang *et al.* [45] learn attention weights for each snippet and then threshold the attention weights for action proposals, which is extended by Nguyen *et al.* [34] with class-agnostic attention mechanism and sparsity constraints. Some methods [43,54,11] try to reduce the classifier’s dependence on specific snippets via masking out them. Several works [38,7,12,31,57] propose a co-action similarity learning to enclose the video-level features between the video pairs with common classes. Shi *et al.* [40] and Luo *et al.* [28] learn the attention weights via variational auto-encoder and expectation-maximization strategy, respectively. Some works [23,18,11,35] seek to explicitly model the background activity for better foreground-background separation. Some works pursue the modality-wise consensus [56,50,32,14] for consistent predictions, which is extended by Hong *et al.* [8] for pre-extracted features re-calibration via cross-modal consensus mechanism. Besides, Lee *et al.* model the background uncertainty on feature magnitude, while Huang *et al.* explore foreground-action consistency.

Though the works mentioned above make great progress, their performances are still highly inferior when compared with fully-supervised action localization approaches. To address this issue, external information is utilized in many works, including external modalities [17,58], external annotation [33,29], external training data [13]. In contrast, we mine the hierarchical supervision and consistency for better action localization without bells and whistles. Besides video-level mining, *i.e.*, multiple instance learning and co-action similarity learning, we introduce snippet-level complementary label learning and snippet-level foreground-background collaborative learning for more correct and consistent predictions. In Sec.4, the efficacy of the proposed HiM-Net is comprehensively verified.

## 3 Methodology

In this section, we first formulate the weakly supervised action localization task (Sec.3.1), and set up the network pipeline for weakly-supervised action localiza-

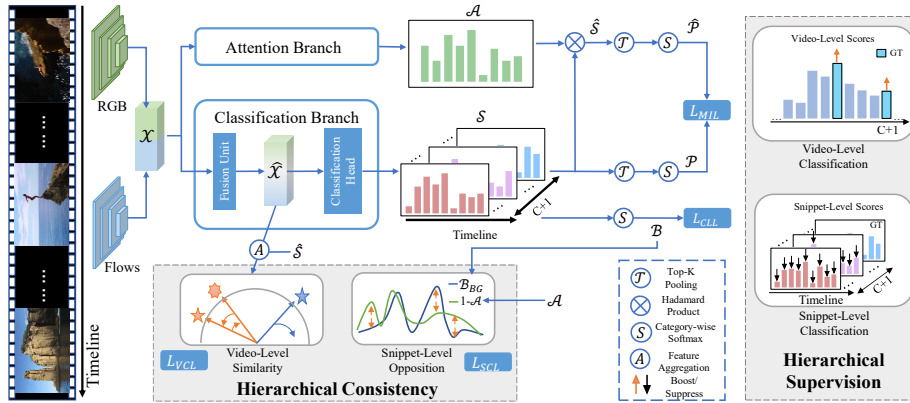


Fig. 2: The workflow of HiM-Net. Given features  $\mathcal{X}$ , HiM-Net generates attention weights  $\mathcal{A}$  and class activation map  $\mathcal{S}$ . Then,  $\mathcal{A}$  suppress the background context in  $\mathcal{S}$  as  $\hat{\mathcal{S}}$ . Both of them are further aggregated as two video-level predictions  $\mathcal{P}$  and  $\hat{\mathcal{P}}$  guided by multiple instance learning  $L_{MIL}$ . Snippet-level classification map  $\mathcal{B}$  transformed from  $\mathcal{S}$  is optimized by complementary label learning  $L_{CLL}$ . Besides hierarchical supervision mining, the video-level co-action similarity learning  $L_{VCL}$  for fused features  $\mathcal{X}$ , and snippet-level foreground-background collaborative learning  $L_{SCL}$  between  $\mathcal{B}_{BG}$  and  $\mathcal{A}$ , are adopted for hierarchical consistency mining.

tion in Sec.3.2. Then, we mine hierarchical supervision (Sec.3.3) and hierarchical consistency (Sec.3.4) for full use of annotations and prediction-wise consistency. Lastly, the overall objective function and how inference is performed are elaborated in Sec.3.5. The workflow of our method is illustrated in Fig.2.

### 3.1 Problem Formulation

Assume a batch of data  $\mathcal{V} = \{\mathbf{v}^{(i)}\}_{i=1}^{|\mathcal{V}|}$  contains  $|\mathcal{V}|$  videos, with video-level annotations  $[y_1^{(i)}, \dots, y_C^{(i)}]$ . Specifically,  $C$  denotes the number of action categories, and  $y_j^{(i)} = 1$  means at least one instance of the  $j$ -th class is in the video  $\mathbf{v}^{(i)}$ , while  $y_j^{(i)} = 0$  if there is no such instance. Here, the superscripts for video index of all symbols are omitted for convenience, *e.g.*,  $\mathbf{v}$  will replace  $\mathbf{v}^{(i)}$ . In WSAL, the goal is to train a model that predicts a set of proposals marked as  $(t_s, t_e, \psi, c)$  in the inference stage. Among the tuples,  $t_s$  and  $t_e$  are the start and end frames of an action instance,  $c$  is the action label, and  $\psi$  represents the confidence.

### 3.2 Main Pipeline

HiM-Net is a two-branch network, including an attention branch and a classification branch. Given the concatenated features  $\mathcal{X} \in \mathbb{R}^{T \times 2D}$  with  $T$  snippets for a video, the attention branch predicts the snippet-level attention map

$\mathcal{A} = [a_1, a_2, \dots, a_T] \in \mathbb{R}^{T \times 1}$ , conveying the class-agnostic foreground probabilities. In the classification branch, input features  $\mathcal{X}$  are first encoded as fused features  $\hat{\mathcal{X}} = [\hat{x}_1, \hat{x}_2, \dots, \hat{x}_T] \in \mathbb{R}^{T \times 2D}$  via the fusion unit, and then used to predict a snippet-level class activation map  $\mathcal{S}$  by a classification head with external background class [18,11]. Note that,  $\mathcal{S} = \{s_{c,t}\}^{C+1,T} \in \mathbb{R}^{(C+1) \times T}$ , where  $s_{c,t}$  is the activation of  $c$ -th class for  $t$ -th snippet (the  $C+1$ -th class means the background category).

By suppressing the background context in the class activation map  $\mathcal{S}$  via  $\mathcal{A}$ , we can get a background-free class activation map  $\hat{\mathcal{S}} = \{\hat{s}_{c,t}\}^{C+1,T} \in \mathbb{R}^{(C+1) \times T}$ , where  $\hat{s}_{c,t}$  is adopted via  $\hat{s}_{c,t} = s_{c,t} \cdot a_t$ . Following the previous works [11,8,14], we aggregate the top  $k$  activation along the temporal axis for each class and average them to get a video-level activation  $\Gamma = [\gamma_1, \gamma_2, \dots, \gamma_{C+1}] \in \mathbb{R}^{C+1}$ :

$$\gamma_c = \frac{1}{k} \max_{\kappa_c \subset \mathcal{S}[c; :]} \sum_{\forall \tau \in \kappa_c} \tau, \quad (1)$$

where  $\kappa_c$  is the top- $k$  set for  $c$ -th class, *i.e.*,  $|\kappa_c| = k$ . Then  $\Gamma$  is activated via Softmax function as video-level classification scores  $\mathcal{P} = [p_1, p_2, \dots, p_{C+1}] \in \mathbb{R}^{C+1}$ :

$$p_c = \frac{\exp(\gamma_c)}{\sum_j^{C+1} \exp(\gamma_j)}, \quad (2)$$

where  $j = 1, 2, \dots, C+1$ . Similarly, we can get background-free video-level classification scores  $\hat{\mathcal{P}}$  via Equ.1 and Equ.2 with  $\hat{\mathcal{S}}$ . Both video-level classification scores  $\mathcal{P}$  and  $\hat{\mathcal{P}}$  are be guided by video-level multiple instance learning.

Besides the video-level classification scores  $\mathcal{P}$  and  $\hat{\mathcal{P}}$ , we also generate the snippet-level classification scores for fine-grained optimization with complementary label learning detailed in the following subsection. Given a vanilla class activation map  $\mathcal{S}$ , the snippet-level classifications scores  $\mathcal{B} = [b_1, b_2, \dots, b_T] \in \mathbb{R}^{(C+1) \times T}$  can be achieved by category-wise Softmax function as below,

$$b_{c,t} = \frac{\exp(s_{c,t})}{\sum_{j'}^{C+1} \exp(s_{j',t})}, \quad (3)$$

where  $j' = 1, 2, \dots, C+1$  and  $t = 1, 2, \dots, T$ . Though the snippet-level classification scores and the video-level ones are generated differently, optimizing them in a hierarchical way can offer a more correct class activation map, which is utilized to estimate the confidences for all proposals.

With predictions generated as the description above, we further explore hierarchical supervision and consistency mining to facilitate the learning of action classification and foreground-background separation, which is detailed below.

### 3.3 Hierarchical Supervision Mining

The cornerstone of supervised learning is to fully leverage the given annotations, especially for the weakly-supervised learning that has limited information. Previous works mainly develop their framework on MIL-paradigm for video-level

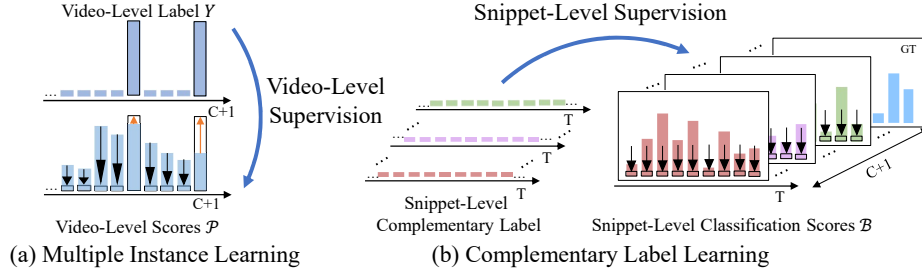


Fig. 3: The illustration of hierarchical supervision mining, which aims to align the predictions with given annotations under video-level and snippet-level manners via multiple instance learning and complementary label learning, respectively.

learning, ignoring the snippet-level one. As shown in Fig.3, the given annotations can be decomposed into video-level labels and snippet-level complementary labels. The former conveys the video-level existence of positive-labeled action categories, the latter indicates the snippet-level inexistence of negative-labeled categories. Intuitively, a perfect prediction should clearly reflect the information in both video-level and snippet-level manners. Thus, we leverage a video-level multiple instance learning and a snippet-level complementary label learning to mine the supervision hierarchically.

**Multiple instance learning.** Given a video  $\mathbf{v}$  annotated with vanilla label  $Y = [y_1, y_2, \dots, y_C] \in \mathbb{R}^C$ . Here, we add an external background label in  $Y$  as  $\bar{Y} = [y_1, \dots, y_C, \bar{y}_{C+1}] \in \mathbb{R}^{C+1}$ , where  $\bar{y}_{C+1} = 1$  represents the existence of background context. Similarly, the background-free label  $\hat{Y} = [y_1, \dots, y_C, \hat{y}_{C+1}] \in \mathbb{R}^{C+1}$ , while  $\hat{y}_{C+1} = 0$  represents the inexistence of background context. As background context exists in every video, optimizing the vanilla video-level classification scores and the background-free ones simultaneously can provide more proper and balanced learning signals for background class. Concretely, with two video-level action scores  $\mathcal{P}$  and  $\hat{\mathcal{P}}$ , the video-level classification loss is derived from Multiple Instance Learning  $L_{MIL}$  as below,

$$L_{MIL} = L_{CCE}(\bar{Y}|\mathcal{P}) + L_{CCE}(\hat{Y}|\hat{\mathcal{P}}), \quad (4)$$

$$L_{CCE}(Y|P) = \frac{1}{C+1} \sum_{c=1}^{C+1} -y_c \log(p_c), \quad (5)$$

where  $L_{CCE}$  is the categorical cross-entropy error function.

**Complementary label learning.** As the video-level multiple instance learning loss  $L_{MIL}$  only conveys video-level constraints by regarding the video as a whole, there may be unexpected high activation for negative-labeled classes

in a specific snippet. That is, the implicit snippet-level learning of  $L_{MIL}$  sub-optimizes snippet-level classification due to the video-level score aggregation as Equ 1 and Equ 2, while the snippet-level classification is closely related with two parts of action localization, *i.e.*, action proposal and confidence estimation.

Remarkably, the given annotations also contain snippet-level inexistence for each negative-labeled class from the perspective of complementary label, which is ignored in previous methods. Partially utilizing the information of given annotations inevitably leads to sub-optimization. To this end, we introduce a snippet-level complementary label learning as a remedy. Given a video with snippet-level classification scores  $\mathcal{B} = [b_1, b_2, \dots, b_T] \in \mathbb{R}^{(C+1) \times T}$  and the video-level label is  $\bar{Y}$ , the complementary label is the inversion as  $1 - \bar{Y}$ . Thus, the snippet-level complementary label learning loss  $L_{CLL}$  can be realized via  $L_{CCE}$  as following to provide fine-grained supervision signals:

$$L_{CLL} = \frac{1}{T} \sum_{b_t \in \mathcal{B}} L_{CCE}(1 - \bar{Y}|1 - b_t). \quad (6)$$

Moreover, the snippet-level classification scores and the video-level ones are achieved via different mechanisms, enabling them to cooperate directly.

### 3.4 Hierarchical Consistency Mining

Besides fully learning the given weak annotations via hierarchical supervision mining, the hierarchical consistency between predictions at any stage is also important for optimizing a precise classifier. Here, the consistency we mined includes video-level co-action similarity learning and the snippet-level foreground-background collaborative learning.

**Video-level co-action similarity learning.** Co-action similarity indicates that identical action should be described similarly, which is mined on the fused features  $\hat{\mathcal{X}} = [\hat{x}_1, \hat{x}_2, \dots, \hat{x}_T] \in \mathbb{R}^{T \times 2D}$  to further enhance the discriminate action representation [38,7,12,8]. Given a video pair  $(\mathbf{v}^{(i)}, \mathbf{v}^{(j)})$  with shared foreground action class  $c$ . To aggregate the categorical-specific video-level features, we first transform the background-free class activation map  $\hat{\mathcal{S}} = [\hat{s}_1, \hat{s}_2, \dots, \hat{s}_T] \in \mathbb{R}^{T \times (C+1)}$  as the temporal weights  $\mathcal{M} = \{\mu_{t,c}\}_{t=1, c=1}^{T, C+1}$  via temporal Softmax function. With the help of the temporal weights, we aggregate the  $c$ -th category-specific video-level foreground feature for  $i$ -th video as  $V_c^i$ , and the corresponding background feature as  $\bar{V}_c^i$ :

$$V_c^i = \sum_{t=1}^T \mu_{t,c} \cdot \hat{x}_{t,c}, \quad \bar{V}_c^i = \frac{1}{\mathcal{T} - 1} \sum_{t=1}^T (1 - \mu_{t,c}) \cdot \hat{x}_{t,c}, \quad (7)$$

where  $\mu_{t,c} = \frac{\exp(\hat{s}_{t,c})}{\sum_{i=1}^{\mathcal{T}} \exp(\hat{s}_{i,c})}$  is the temporal Softmax function. Then, the categorical-specific video-level features for the video pairs  $(\mathbf{v}^{(i)}, \mathbf{v}^{(j)})$  with shared action class



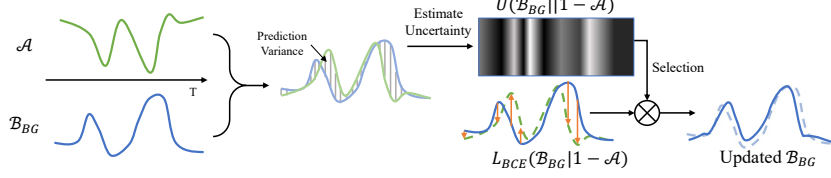


Fig. 4: The illustration of snippet-level foreground-background collaborative learning. Half of the process is shown for convenience, while the other part for  $\mathcal{A}$  learning works similarly. Here, prediction variance is estimated via  $U(p||q)$  as uncertainty to select the consensus terms for collaborative learning.

$c$  are  $V_c^i$  and  $V_c^j$ . Intuitively, these two category-specific foreground features should be similar, compared with their own video-level background features  $\bar{V}_c^i$  and  $\bar{V}_c^j$ . Here, we adopt  $d(\cdot, \cdot) = 1 - \text{Cos}(\cdot, \cdot)$ , to estimate the feature-wise distance, where  $\text{Cos}(\cdot, \cdot)$  is cosine distance function. By leveraging a margin  $\delta$ ,  $L_{VCL}$  is designed as triplet loss to estimate the video-level similarity as below,

$$L_{VCL} = \frac{1}{2}[d(V_c^i, V_c^j) - d(V_c^i, \bar{V}_c^j) + \delta]_+ + \frac{1}{2}[d(V_c^i, V_c^j) - d(V_c^j, \bar{V}_c^i) + \delta]_+, \quad (8)$$

where  $\delta=0.5$  and  $[\cdot]_+$  is a ReLU function.

**Snippet-level foreground-background collaborative learning.** There are two estimations from two different branches of our HiM-Net, *i.e.*,  $\mathcal{A}$  and  $\mathcal{B}_{BG} = \mathcal{B}_{C+1}$  representing foreground and background, respectively. Intuitively, the foreground and background estimations should be opposite to each other. As shown in Fig.4, we treat two estimations as other’s pseudo targets, to mine the snippet-level consistency between them. Considering the label noise is inevitable in both estimations, aligning them directly will excessively focus on the mutually different parts, leading to noise amplification and instabilities. Intuitively, if two noisy estimations achieve consensus for a specific snippet as “foreground” or “background”, it’s more likely to be right. Thus, without introducing external parameter or complex training process, we use their prediction variance as the uncertainty to filter out the non-consensus term. More concretely, Kullback–Leibler ( $D_{KL}$ ) divergence is used to estimate the prediction variance [62]. Remarkably, we use the  $D_{KL}(q||p)$  to estimate the **self-centered variance** from predicted result  $p$  to the pseudo target  $q$ , to select the items with high consensus for  $p$  asymmetrically. As  $D_{KL}(q||p) \geq 0$ , an exponential function is employed to generate the uncertainty term as  $U(p||q) \in (0, 1]$ ,

$$U(p||q) = \exp[-\alpha \cdot D_{KL}(q||p)] = \exp[-\alpha \cdot p \log(\frac{p}{q})], \quad (9)$$

where  $\alpha$  is a hyperparameter to control the uncertainty weight generation. The weights for the non-consensus terms will go down when  $\alpha$  gets higher. Remarkably, when  $\alpha = 0$ , the uncertainty term in Equ.9 will degenerate as constant

value 1 with no selection capacity. Then, we get the foreground-background collaborative learning loss  $L_{SCL}$ ,

$$L_{SCL} = \sum_{t=1}^T U(1 - a_t | b_t) \cdot L_{BCE}(b_t | 1 - a_t) + \sum_{t=1}^T U(a_t | 1 - b_t) \cdot L_{BCE}(a_t | 1 - b_t), \quad (10)$$

where  $L_{BCE}$  is the binary cross-entropy error function. As  $L_{BCE}$  can reduce the variance,  $U(p|q)$  will not be too small, avoiding the mode collapse. Thus, leveraging the uncertainty term  $U(p|q)$ , two estimations select the self-centered consensus items to promote themselves adaptively.

### 3.5 Overall Objective Function and Inference

Overall, we combine all the loss functions mentioned above to form our final objective function to mine hierarchical supervision and consistency:

$$L = L_{MIL} + L_{CCL} + \lambda_1 L_{VCL} + \lambda_2 L_{SCL}, \quad (11)$$

where hyperparameters  $\lambda_1, \lambda_2$  control the hierarchical consistency mining.

After learning with hierarchical mining strategy, a well-trained model is derived. To generate action proposals for the given video during inference, concatenated features are fed into HiM-Net and obtain  $\mathcal{A}$  and  $\hat{\mathcal{S}}$ . The class-agnostic action proposals are obtained by selecting the one-dimensional connected components from  $\mathcal{A}$  via multiple thresholds. We denote the candidate action instance as  $\{(t_s, t_e, \psi, c)\}$ , where  $\psi$  is the proposal-level classification score (*i.e.*, outer-inner contrastive score [41]) for class  $c$ . Note that, to enrich the proposal set, we adopt multiple thresholds for proposal generation, and then remove the redundant overlapping instances via non-maximization suppression.

## 4 Experiments

### 4.1 Experimental Settings

We evaluate our method on two public benchmarks datasets, *i.e.*, THUMOS14 [15] and ActivityNet1.3 [2], for temporal action localization.

- **THUMOS14** dataset contains 200 validation videos and 213 test videos of 20 action classes. It is a very challenging benchmark, whose videos have diverse lengths and frequent action instances. Following the previous works, we treat the validation videos as the training set and the test videos for testing.

- **ActivityNet1.3** is a large dataset that covers 200 action categories, with a training set of 10,024 videos and a validation set of 4,926 videos. We use the training set and validation set for training and testing, respectively.

- **Evaluation metric.** We evaluate our method with mean average precision (mAP) under several different intersections of union (IoU) thresholds, which are

the standard evaluation metrics for temporal action localization. We use the officially released evaluation code<sup>2</sup> to measure our results.

- **Implementation details.** At first, we apply I3D [3] pre-trained on Kinetics-400 [16] to extract both RGB and optical flow features, which are concatenated into 2048-dimensional snippet-level features. Each snippet contains continuous non-overlapping 16 frames. The method is implemented in PyTorch [37]. In the training stage, we uniformly sample 560 snippets for THUMOS14 and 60 snippets for ActivityNet1.3 for each video, while all snippets are taken during evaluation. We randomly sample 10 videos in a batch, where 3 pairs of videos contain the same kind of actions respectively for  $\mathcal{L}_{VCL}$ .  $\lambda_1=1$ ,  $\lambda_2=0.01$ ,  $\alpha=4$ . Adam optimizer with 0.001 weight decay rate and 0.00003 learning rate is used. For THUMOS14, the training stage takes 10000 iterations,  $k=80$ . As for ActivityNet1.3, it takes 20000 iterations and  $k=6$ . All experiments are performed on an NVIDIA GTX 1080Ti GPU. More details are available in *Supplementary*.

## 4.2 Comparisons with state-of-the-art methods

HiM-Net is compared with the existing weakly-supervised methods and fully-supervised methods on THUMOS14 under several IoU thresholds with NMS and Soft-NMS [1] post-processing operations, which are reported in Table 1. We separate the horizontal blocks regarding the levels of supervision. HiM-Net achieves comparable or the best results in terms of the average mAP over almost IoU thresholds in WSAL, regardless of the post-processing operation. Moreover, HiM-Net outperforms those explicitly modeling the background context [18,11,8] and those who mine the video-level co-action similarity [57,8], which verifies the snippet-level mining can help our HiM-Net perform better. Without bells and whistles, HiM-Net outperforms the methods that introduce external data or annotation, showing the necessity to mine hierarchical supervision and consistency. Additionally, the results of HiM-Net are even comparable with fully-supervised in terms of mAP@0.1 and mAP@0.2, and better than [61]. The visualization for detection scores of HiM-Net is also reported on THUMOS14 in Fig.8.

We also report our results evaluated on ActivityNet1.3 in Tab.2. Consistent with the results on THUMOS14, our method also achieves the best performance on almost all terms for the ActivityNet1.3, indicating the efficacy of hierarchical mining in improving the action detection.

## 4.3 Ablation study

Here, a set of ablation studies are conducted on THUMOS14 to analyze the efficacy of each component in HiM-Net. The results of ablation studies for all the loss functions are shown in Tab.3, where we perform the experiments multiple times with different seeds to report the mean values and corresponding standard variances. We use ‘‘AVG’’ for the performance metric, which is the average of mAP values for different IoU thresholds (0.1:0.1:0.7). Besides, the snippet-level

<sup>2</sup> <http://github.com/activitynet/ActivityNet>

Supervision	Method	Year	Post-Processing	mAP@IoU (%)							AVG 0.1:0.5
				0.1	0.2	0.3	0.4	0.5	0.6	0.7	
Full	SSN [61]	2017	NMS	60.3	56.2	50.6	40.8	29.1	-	-	47.4
	BSN [22]	2018	Soft-NMS	-	-	53.5	45.0	36.9	28.4	20.0	-
	BMN [20]	2019	Soft-NMS	-	-	56.0	47.4	38.8	29.7	20.5	-
	P-GCN [55]	2019	Soft-NMS	69.5	67.8	63.6	57.8	49.1	-	-	61.6
Weak†	STAR [48]	2019	NMS	68.8	60.0	48.7	34.7	23.0	-	-	47.0
	3C-NET [33]	2019	NMS	59.1	53.5	44.2	34.1	26.6	-	8.1	43.5
	PreTrimNet [58]	2020	NMS	57.5	50.7	41.4	32.1	23.1	14.2	7.7	41.0
	SF-Net [29]	2020	NMS	71.0	63.4	53.2	40.7	29.3	18.4	9.6	51.5
Weak	BaS-Net [18]	2020	NMS	58.2	52.3	44.6	36.0	27.0	18.6	10.4	43.6
	EM-MIL [28]	2020	NMS	59.1	52.7	45.5	36.8	30.5	22.7	16.4	44.9
	A2CL-PT [31]	2020	NMS	61.2	56.1	48.1	39.0	30.1	19.2	10.6	46.9
	TSCN [56]	2020	NMS	63.4	57.6	47.8	37.7	28.7	19.4	10.2	47.0
	UM [19]	2021	NMS	67.5	61.2	52.3	43.4	33.7	22.9	12.1	51.6
	CoLA [57]	2021	NMS	66.2	59.5	51.5	41.9	32.2	22.0	13.1	50.3
	AUMN [27]	2021	NMS	66.2	61.9	54.9	44.4	33.3	20.5	9.0	52.1
	FAC-Net [10]	2021	NMS	67.6	62.1	52.6	44.3	33.4	22.5	12.7	52.0
	D2-Net [32]	2021	NMS	65.7	60.2	52.3	43.4	36.0	-	-	51.5
	ACGNet [52]	2022	NMS	68.1	62.6	53.1	44.6	34.7	22.6	12.0	52.6
	<b>HiM-Net</b>	<b>Ours</b>	<b>NMS</b>	<b>70.6</b>	<b>65.3</b>	<b>55.9</b>	<b>45.1</b>	<b>35.7</b>	<b>21.8</b>	<b>10.8</b>	<b>54.5</b>
	HAM-Net [11]	2021	Soft-NMS	65.4	59.0	50.3	41.1	31.0	20.7	11.1	49.4
	ASL [30]	2021	Soft-NMS	67.0	-	51.8	-	31.1	-	11.4	-
	CSCL [14]	2021	Soft-NMS	68.0	61.8	52.7	43.3	33.4	21.8	12.3	51.8
CO <sub>2</sub> -Net [8]	2021	Soft-NMS	70.1	63.6	54.5	45.7	38.3	26.4	13.4	54.4	
<b>HiM-Net</b>	<b>Ours</b>	<b>Soft-NMS</b>	<b>70.4</b>	<b>65.0</b>	<b>55.8</b>	<b>46.7</b>	<b>37.8</b>	<b>25.7</b>	<b>14.0</b>	<b>55.2</b>	

Table 1: Comparisons on the THUMOS14 with NMS and Soft-NMS post-processing. AVG is the average mAP under thresholds 0.1:0.1:0.5; while † means using additional information, *e.g.* frequency or pose.

classification accuracy is also estimated by “ACC”. Exp.1 is the baseline only trained with  $L_{MIL}$ , while Exp.4 is our full method. All the reported results show that all the designed loss components are required to maximize the performance. Besides, we also visualize some qualitative results for some loss function combinations in Fig.5, which verify hierarchical mining can suppress the unexpected activation for better action localization.

**- Effect of Complementary Label Learning.** As shown in Tab.3, taking the Exp.1 trained with  $L_{MIL}$  as baseline, the average mAP gets great improvement as high as +4.4% on average mAP with the assistance of  $L_{CLL}$ , and the snippet-level classification gets improved by 16.1%. Moreover, when training without  $L_{CLL}$ , the action localization performance gets 2.9% depression, and the snippet-level classification goes down about 7%. These results clearly verify that learning from the snippet-level complementary labels enables HiM-Net to suppress the unexpected activation for all snippets in unlabeled classes, improving the snippet-level classification and action localization.

**- Effect of Foreground-background Collaborative Learning.** As shown in Tab.3, with the help of  $L_{SCL}$ , Exp.4 surpasses Exp.3 by 0.7% on action localization performance, the snippet-level classification performance also gets improved. In addition, we conducted multiple ablation studies on the  $L_{SCL}$ . Compared with existing foreground-background mutual learning loss  $L_{guide}$  [11,8] and  $L_{ml}$  [8], using  $L_{SCL}$  gets much better action localization performance with growth of 0.8% on “AVG” mAP as well as better foreground-background separation

Supervision	Method	Year	Post-processing	0.5	0.75	0.95	AVG mAP
Full	TAL-Net [4]	2018	NMS	38.2	18.3	1.3	20.2
	BSN [22]	2018	Soft-NMS	46.5	30.0	8.0	30.0
	P-GCN [55]	2019	Soft-NMS	42.9	28.1	2.5	27.0
Weak <sup>†</sup>	TSRNet [59]	2019	NMS	33.1	18.7	3.3	21.8
	STAR [48]	2019	NMS	31.1	18.8	4.7	-
	PreTrimNet [58]	2020	NMS	34.8	20.9	5.3	22.5
Weak	BaS-Net [18]	2020	NMS	34.5	22.5	4.9	22.2
	A2CL-PT [31]	2020	NMS	36.8	22.0	5.2	22.5
	TSCN [56]	2020	NMS	35.3	21.4	5.3	21.7
	ACSNet [25]	2021	NMS	36.3	24.2	5.8	23.9
	UM [19]	2021	NMS	37.0	23.9	5.7	23.7
	AUMN [27]	2021	NMS	38.3	23.5	5.2	23.5
	UGCT [50]	2021	NMS	39.1	22.4	5.8	23.8
	FAC-Net [10]	2021	NMS	37.6	24.2	6.0	24.0
	<b>HiM-Net</b>	<b>Ours</b>	<b>NMS</b>	<b>38.6</b>	<b>25.2</b>	<b>5.6</b>	<b>24.8</b>
	<b>HiM-Net</b>	<b>Ours</b>	<b>Soft-NMS</b>	<b>40.8</b>	<b>25.6</b>	<b>6.0</b>	<b>25.6</b>

Table 2: Comparisons between HiM-Net with other methods on the ActivityNet1.3 dataset. <sup>†</sup> indicates the use of additional information. AVG mAP means average mAP from IoU 0.5 to 0.95 with 0.05 increment.

Exp	$L_{MIL}$	$L_{CLL}$	$L_{VCL}$	$L_{SCL}$	AVG	ACC
1	✓				39.3±0.6	61.7±0.9
2	✓	✓			43.7±0.2	77.8±0.4
3	✓	✓	✓		44.4±0.1	78.6±0.1
4	✓	✓	✓	✓	<b>45.1±0.1</b>	<b>78.7±0.1</b>
5	✓	✓	✓	✓	43.7±0.1	77.7±0.2
6	✓		✓	✓	42.2±0.3	71.5±0.3
7	✓		✓		41.7±0.5	71.4±1.0
8	✓			✓	42.6±0.3	74.1±0.2

Table 3: Ablation studies on THU-MOS14. AVG is the average mAP for IoU thresholds 0.1:0.7. ACC is snippet-level classification accuracy of  $\mathcal{S}$ .

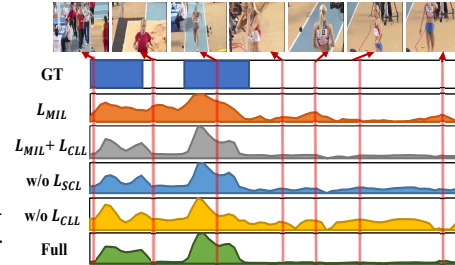


Fig. 5: The qualitative results of ablation studies on a video of THUMOS14.

performance represented on snippet-level foreground-background classification accuracy. If  $L_{SCL}$  has no uncertainty term  $U(p||q)$  or uses the variant target-centered uncertainty term  $U(q||p)$ , the label noise hinder the optimization, showing that self-centered uncertainty term  $U(p||q)$  is more capable in selecting the consensus terms. As for the value selection for hyperparameter  $\alpha$ , we report the results with varying  $\alpha$  from 0.5 to 10 on THUMOS14 in Fig.6, where the best performance is got when  $\alpha=4$ . When  $\alpha$  gets even larger, the model seems to overfit on the consensus terms with clear performance drops. In Fig.7, we use KDE (kernel density distribution) to visualize the estimated uncertainty distribution for background snippets from the models training with or without  $L_{SCL}$ . As shown in Fig.7 and Tab.3, training with  $L_{SCL}$  helps the background snippets to be separated more correctly with more consensus.

- **The generality of  $L_{CLL}$  and  $L_{SCL}$ .** In addition, we also verify the generality of  $L_{CLL}$  and  $L_{SCL}$  on existing methods with explicit background modeling, *i.e.*, BaS-Net [18] and HAM-Net [11], which are reported in Tab.5. Applying  $L_{CLL}$  or  $L_{SCL}$  can boost up their performance by around or over 1%, showing the generality and efficacy of  $L_{CLL}$ . Specifically, compared with the use of  $L_{BCE}$  for

Method	0.1	0.3	0.5	0.7	AVG	ACC
$L_{guide}$ [11]	70.3	55.8	37.3	13.3	44.3	80.1
$L_{mi}$ [8]	70.2	55.4	36.9	13.8	44.3	76.6
w/o $L_{SCL}$	70.1	55.2	37.0	13.5	44.4	80.1
$L_{SCL}$ w/o $U(p q)$	69.8	55.4	38.1	14.1	44.8	80.1
$L_{SCL}$ with $U(q p)$	70.2	56.0	37.7	13.4	44.8	79.7
$L_{SCL}$	<b>70.4</b>	<b>55.8</b>	<b>37.8</b>	<b>14.0</b>	<b>45.1</b>	<b>80.3</b>

Table 4: Ablation studies of  $L_{SCL}$  on THUMOS14. AVG is the average mAP under multiple thresholds 0.1:0.7. ACC is the snippet-level foreground-background classification accuracy.

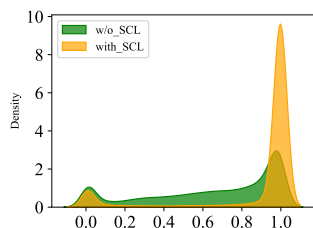


Fig. 7: Uncertainty distribution for background snippets from the models training with  $L_{SCL}$  (orange) or without (green).

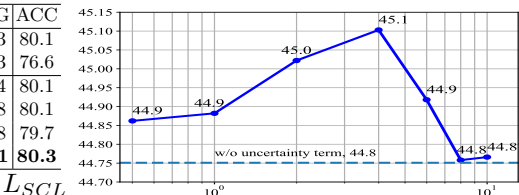


Fig. 6: Analysis of the hyperparameter  $\alpha$  on THUMOS14. We report the average mAPs under IoU thresholds 0.1:0.7 with varying  $\alpha$  from 0.5 to 10.

Method	0.1	0.3	0.5	0.7	AVG	$\Delta$
BaS-Net	56.5	43.1	26.0	9.9	34.1	-
+ $L_{CLL}$	59.6	45.4	29.6	10.0	36.4	<b>+2.3</b>
+ $L_{CLL}$ + $L_{SCL}$	60.5	46.9	31.5	11.3	37.8	<b>+3.7</b>
HAM-Net	65.4	50.3	31.0	11.1	39.8	-
+ $L_{CLL}$	66.9	51.3	32.4	12.2	40.9	<b>+1.1</b>
+ $L_{SCL}$	66.1	51.8	31.8	11.8	40.7	<b>+0.9</b>

Table 5: Applying  $L_{CLL}$  and  $L_{SCL}$  on other frameworks with explicit background modeling, *i.e.*, BaS-Net [18] and HAM-Net[11]. “AVG” is the average mAP under IoU thresholds 0.1:0.7; “ $\Delta$ ” is the gains.

video-level multiple instance learning [18], learning with  $L_{CLL}$  additionally is much better, showing the reasonability in introducing snippet-level supervision mining.

#### 4.4 Qualitative Results

To confirm the superiority of our hierarchical mining, we qualitatively visualize the results on THUMOS14 in Fig.8. From the figure, we can find out that most of the action instances are well localized with high activation, while attention map  $\mathcal{A}$  and snippet-level background classification scores  $\mathcal{B}_{BG}$  are predicted oppositely, showing the high consensus. Moreover, the qualitative results of ablation studies are shown in Fig.5. By comparing  $L_{MIL}$  with  $L_{MIL} + L_{CLL}$ , and “Full” with w/o  $L_{CLL}$ , we can find out the unexpected activation are well suppressed with  $L_{CLL}$ , generating correct action proposals.

## 5 Conclusions

In this work, we aim to relieve the limited supervision restriction for weakly-supervised action localization by hierarchically mining the supervision from the weak annotations and prediction-wise consistency. Specifically, two snippet-level

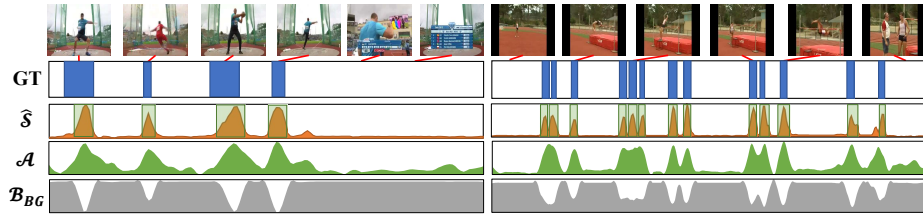


Fig. 8: Qualitative results on THUMOS14. The horizontal axis denotes time. GT (blue) means the ground truth, while the orange is class activation map  $\hat{\mathcal{S}}$ , and the green boxes are the proposals. The bottom two bars are attention  $\mathcal{A}$  (green) and snippet-level background classification scores  $\mathcal{B}_{BG}$  (gray), respectively.

mining strategies are proposed: a complementary label learning to mine the snippet-level supervision for precise suppression on unexpected activation, and an uncertainty-aware foreground-background collaborative learning for mutual promoting the foreground-background separation by mining the snippet-level consistency. Verified by massive experimental results on THUMOS14 and ActivityNet1.3 benchmarks, hierarchical mining relieves the restriction to some degree and helps our method achieve a new state-of-the-art.

## References

1. Bodla, N., Singh, B., Chellappa, R., Davis, L.S.: Soft-nms—improving object detection with one line of code. In: ICCV (2017)
2. Caba Heilbron, F., Escorcia, V., Ghanem, B., Carlos Niebles, J.: Activitynet: A large-scale video benchmark for human activity understanding. In: CVPR (2015)
3. Carreira, J., Zisserman, A.: Quo vadis, action recognition? a new model and the kinetics dataset. In: CVPR (2017)
4. Chao, Y.W., Vijayanarasimhan, S., Seybold, B., Ross, D.A., Deng, J., Sukthankar, R.: Rethinking the faster r-cnn architecture for temporal action localization. In: CVPR (2018)
5. Feng, J.C., Hong, F.T., Zheng, W.S.: Mist: Multiple instance self-training framework for video anomaly detection. In: CVPR (2021)
6. Gao, J., Yang, Z., Chen, K., Sun, C., Nevatia, R.: Turn tap: Temporal unit regression network for temporal action proposals. In: ICCV (2017)
7. Gong, G., Wang, X., Mu, Y., Tian, Q.: Learning temporal co-attention models for unsupervised video action localization. In: CVPR (2020)
8. Hong, F.T., Feng, J.C., Xu, D., Shan, Y., Zheng, W.S.: Cross-modal consensus network for weakly supervised temporal action localization. In: ACM MM (2021)
9. Hong, F.T., Huang, X., Li, W.H., Zheng, W.S.: Mini-net: Multiple instance ranking network for video highlight detection. In: ECCV (2020)
10. Huang, L., Wang, L., Li, H.: Foreground-action consistency network for weakly supervised temporal action localization. In: ICCV (2021)
11. Islam, A., Long, C., Radke, R.: A hybrid attention mechanism for weakly-supervised temporal action localization. In: AAAI (2021)
12. Islam, A., Radke, R.: Weakly supervised temporal action localization using deep metric learning. In: WACV (2020)
13. Jain, M., Ghodrati, A., Snoek, C.G.: Actionbytes: Learning from trimmed videos to localize actions. In: CVPR (2020)
14. Ji, Y., Jia, X., Lu, H., Ruan, X.: Weakly-supervised temporal action localization via cross-stream collaborative learning. In: ACM MM (2021)
15. Jiang, Y.G., Liu, J., Roshan Zamir, A., Toderici, G., Laptev, I., Shah, M., Sukthankar, R.: THUMOS challenge: Action recognition with a large number of classes. <http://csrcv.ucf.edu/THUMOS14/> (2014)
16. Kay, W., Carreira, J., Simonyan, K., Zhang, B., Hillier, C., Vijayanarasimhan, S., Viola, F., Green, T., Back, T., Natsev, P., et al.: The kinetics human action video dataset. arXiv (2017)
17. Lee, J.T., Jain, M., Park, H., Yun, S.: Cross-attentional audio-visual fusion for weakly-supervised action localization. In: ICLR (2020)
18. Lee, P., Uh, Y., Byun, H.: Background suppression network for weakly-supervised temporal action localization. In: AAAI (2020)
19. Lee, P., Wang, J., Lu, Y., Byun, H.: Weakly-supervised temporal action localization by uncertainty modeling. In: AAAI (2021)
20. Lin, T., Liu, X., Li, X., Ding, E., Wen, S.: Bmn: Boundary-matching network for temporal action proposal generation. In: ICCV (2019)
21. Lin, T., Zhao, X., Shou, Z.: Single shot temporal action detection. In: ACM MM (2017)
22. Lin, T., Zhao, X., Su, H., Wang, C., Yang, M.: Bsn: Boundary sensitive network for temporal action proposal generation. In: ECCV (2018)



23. Liu, D., Jiang, T., Wang, Y.: Completeness modeling and context separation for weakly supervised temporal action localization. In: CVPR (2019)
24. Liu, X., Lee, J.Y., Jin, H.: Learning video representations from correspondence proposals. In: CVPR (2019)
25. Liu, Z., Wang, L., Zhang, Q., Tang, W., Yuan, J., Zheng, N., Hua, G.: Acenet: Action-context separation network for weakly supervised temporal action localization. In: AAAI (2021)
26. Long, F., Yao, T., Qiu, Z., Tian, X., Luo, J., Mei, T.: Gaussian temporal awareness networks for action localization. In: CVPR (2019)
27. Luo, W., Zhang, T., Yang, W., Liu, J., Mei, T., Wu, F., Zhang, Y.: Action unit memory network for weakly supervised temporal action localization. In: CVPR (2021)
28. Luo, Z., Guillory, D., Shi, B., Ke, W., Wan, F., Darrell, T., Xu, H.: Weakly-supervised action localization with expectation-maximization multi-instance learning. In: ECCV (2020)
29. Ma, F., Zhu, L., Yang, Y., Zha, S., Kundu, G., Feiszli, M., Shou, Z.: Sf-net: Single-frame supervision for temporal action localization. In: ECCV (2020)
30. Ma, J., Gorti, S.K., Volkovs, M., Yu, G.: Weakly supervised action selection learning in video. In: CVPR (2021)
31. Min, K., Corso, J.J.: Adversarial background-aware loss for weakly-supervised temporal activity localization. In: ECCV (2020)
32. Narayan, S., Cholakkal, H., Hayat, M., Khan, F.S., Yang, M.H., Shao, L.: D2-net: Weakly-supervised action localization via discriminative embeddings and denoised activations. In: ICCV (2021)
33. Narayan, S., Cholakkal, H., Khan, F.S., Shao, L.: 3c-net: Category count and center loss for weakly-supervised action localization. In: ICCV (2019)
34. Nguyen, P., Liu, T., Prasad, G., Han, B.: Weakly supervised action localization by sparse temporal pooling network. In: CVPR (2018)
35. Nguyen, P.X., Ramanan, D., Fowlkes, C.C.: Weakly-supervised action localization with background modeling. In: ICCV (2019)
36. Pardo, A., Alwassel, H., Caba, F., Thabet, A., Ghanem, B.: Refineloc: Iterative refinement for weakly-supervised action localization. In: WACV (2021)
37. Paszke, A., Gross, S., Massa, F., Lerer, A., Bradbury, J., Chanan, G., Killeen, T., Lin, Z., Gimselshein, N., Antiga, L., et al.: Pytorch: An imperative style, high-performance deep learning library. NeurIPS (2019)
38. Paul, S., Roy, S., Roy-Chowdhury, A.K.: W-talc: Weakly-supervised temporal activity localization and classification. In: ECCV (2018)
39. Qing, Z., Su, H., Gan, W., Wang, D., Wu, W., Wang, X., Qiao, Y., Yan, J., Gao, C., Sang, N.: Temporal context aggregation network for temporal action proposal refinement. In: CVPR (2021)
40. Shi, B., Dai, Q., Mu, Y., Wang, J.: Weakly-supervised action localization by generative attention modeling. In: CVPR (2020)
41. Shou, Z., Gao, H., Zhang, L., Miyazawa, K., Chang, S.F.: Autoloc: Weakly-supervised temporal action localization in untrimmed videos. In: ECCV (2018)
42. Shou, Z., Wang, D., Chang, S.F.: Temporal action localization in untrimmed videos via multi-stage cnns. In: CVPR (2016)
43. Singh, K.K., Lee, Y.J.: Hide-and-peek: Forcing a network to be meticulous for weakly-supervised object and action localization. In: ICCV (2017)
44. Tian, Y., Pang, G., Chen, Y., Singh, R., Verjans, J.W., Carneiro, G.: Weakly-supervised video anomaly detection with robust temporal feature magnitude learning. In: ICCV (2021)

45. Wang, L., Xiong, Y., Lin, D., Van Gool, L.: Untrimmednets for weakly supervised action recognition and detection. In: CVPR (2017)
46. Xiong, B., Kalantidis, Y., Ghadiyaram, D., Grauman, K.: Less is more: Learning highlight detection from video duration. In: CVPR (2019)
47. Xu, M., Zhao, C., Rojas, D.S., Thabet, A., Ghanem, B.: G-tad: Sub-graph localization for temporal action detection. In: CVPR (2020)
48. Xu, Y., Zhang, C., Cheng, Z., Xie, J., Niu, Y., Pu, S., Wu, F.: Segregated temporal assembly recurrent networks for weakly supervised multiple action detection. In: AAAI (2019)
49. Yang, L., Peng, H., Zhang, D., Fu, J., Han, J.: Revisiting anchor mechanisms for temporal action localization. TIP **29** (2020)
50. Yang, W., Zhang, T., Yu, X., Qi, T., Zhang, Y., Wu, F.: Uncertainty guided collaborative training for weakly supervised temporal action detection. In: CVPR (2021)
51. Yang, W., Zhang, T., Zhang, Y., Wu, F.: Local correspondence network for weakly supervised temporal sentence grounding. TIP **30** (2021)
52. Yang, Z., Qin, J., Huang, D.: Acgnet: Action complement graph network for weakly-supervised temporal action localization. arXiv (2021)
53. Yuan, Z., Stroud, J.C., Lu, T., Deng, J.: Temporal action localization by structured maximal sums. In: CVPR (2017)
54. Zeng, R., Gan, C., Chen, P., Huang, W., Wu, Q., Tan, M.: Breaking winner-takes-all: Iterative-winners-out networks for weakly supervised temporal action localization. TIP (2019)
55. Zeng, R., Huang, W., Tan, M., Rong, Y., Zhao, P., Huang, J., Gan, C.: Graph convolutional networks for temporal action localization. In: ICCV (2019)
56. Zhai, Y., Wang, L., Tang, W., Zhang, Q., Yuan, J., Hua, G.: Two-stream consensus network for weakly-supervised temporal action localization. In: ECCV (2020)
57. Zhang, C., Cao, M., Yang, D., Chen, J., Zou, Y.: Cola: Weakly-supervised temporal action localization with snippet contrastive learning. In: CVPR (2021)
58. Zhang, X.Y., Shi, H., Li, C., Li, P.: Multi-instance multi-label action recognition and localization based on spatio-temporal pre-trimming for untrimmed videos. In: AAAI (2020)
59. Zhang, X.Y., Shi, H., Li, C., Zheng, K., Zhu, X., Duan, L.: Learning transferable self-attentive representations for action recognition in untrimmed videos with weak supervision. In: AAAI. vol. 33 (2019)
60. Zhang, Z., Zhao, Z., Lin, Z., He, X., et al.: Counterfactual contrastive learning for weakly-supervised vision-language grounding. NeurIPS **33** (2020)
61. Zhao, Y., Xiong, Y., Wang, L., Wu, Z., Tang, X., Lin, D.: Temporal action detection with structured segment networks. In: ICCV (2017)
62. Zheng, Z., Yang, Y.: Rectifying pseudo label learning via uncertainty estimation for domain adaptive semantic segmentation. IJCV **129**(4) (2021)
63. Zhong, J.X., Li, N., Kong, W., Liu, S., Li, T.H., Li, G.: Graph convolutional label noise cleaner: Train a plug-and-play action classifier for anomaly detection. In: CVPR (2019)
64. Zhong, J.X., Li, N., Kong, W., Zhang, T., Li, T.H., Li, G.: Step-by-step erasion, one-by-one collection: a weakly supervised temporal action detector. In: ACM MM (2018)
65. Zhou, Z.H.: Multi-instance learning: A survey. Department of Computer Science & Technology, Nanjing University, Tech. Rep **1** (2004)